Available online at www.sciencedirect.com
SCIENCE DIRECT®
Coordination Chemistry Reviews 238–239 (2003) 233–253
COORDINATION CHEMISTRY REVIEWS
www.elsevier.com/locate/ccr

Molecular orbital and DFT studies on water exchange mechanisms of metal ions

Hans Erras-Hanauer [a,b], Timothy Clark [b,*], Rudi van Eldik [a,*]

[a] *Institute for Inorganic Chemistry, University of Erlangen-Nürnberg, Egerlandstrasse 1, 91058 Erlangen, Germany*
[b] *Computer Chemistry Centre, University of Erlangen-Nürnberg, Nägelsbachstrasse 25, 91052 Erlangen, Germany*

Received 1 May 2002; accepted 11 October 2002

Contents

Abstract

An overview of recent molecular orbital theory and density functional theory studies on water exchange reactions of metal ions and complexes in solution is presented. The different theoretical techniques used are reviewed and representative examples are discussed. The mechanistic insight gained is discussed in reference to available experimental data and the predictive nature of the applied techniques is highlighted.

Keywords: Molecular orbital; DFT studies; Water exchange mechanisms

* Corresponding authors. Tel.: +49-9131-852-7350; fax: +49-9131-852-7387
E-mail address: vaneldik@chemie.uni-erlangen.de (R. van Eldik), clark@chemie.uni-erlangen.de (T. Clark).

0010-8545/02/$ - see front matter © 2002 Elsevier Science B.V. All rights reserved.
PII: S0010-8545(02)00296-5

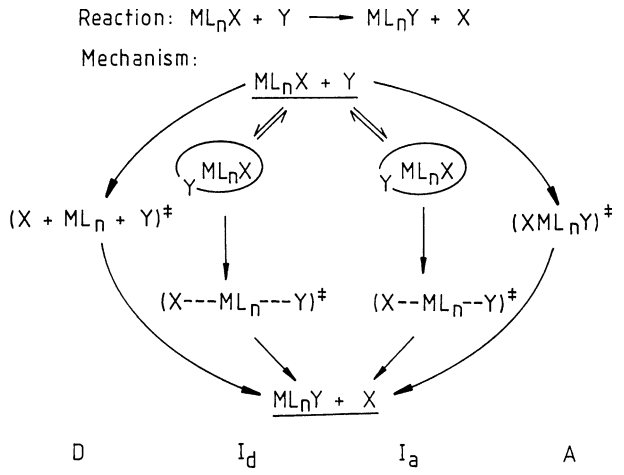

Fig. 1. Schematic presentation of the possible ligand substitution mechanisms.

1. Introduction

Ligand substitution reactions of metal complexes have been the topic of many mechanistic studies in coordination chemistry because of the fundamental role of such reactions in many chemical, biological and catalytic processes. For a general ligand substitution reaction (1):

$$ML_nX + Y \rightarrow ML_nY + X \quad (1)$$

where X is the leaving group, Y the entering ligand, and L_n the spectator ligand(s) (charges are omitted for clarity). There are basically three simple pathways: (i) the dissociative (D) process with an intermediate of lower coordination number; (ii) the associative (A) process with an intermediate of higher coordination number; (iii) the interchange (I) process, in which no intermediate of lower or higher coordination number is involved. The interchange of the ligands X and Y can be more dissociative (I_d) or more associative (I_a) in nature, depending on whether bond breakage or bond formation is more important, respectively. These mechanisms are outlined schematically in Fig. 1.

In the case of the limiting D and A mechanisms, the transition states indicate the degree of bond breakage or bond formation, respectively. For the interchange mechanisms I_d and I_a, the reactants have been suggested to form a precursor complex in a rapid pre-equilibration prior to the rate-determining interchange of X and Y.

Such ligand substitution reactions should exhibit very characteristic volume of activation data depending on the degree of bond breakage or bond formation in the transition state. The simplest type of ligand substitution reaction involves the symmetrical exchange of coordinated solvent or ligand with bulk solvent or ligand molecules, respectively.

$$[M(S)_x]^{n+} + S^* \rightarrow [M(S)_{x-1}(S^*)]^{n+} + S \quad (2)$$

Exchange of a unidentate solvent molecule (S) between the first coordination sphere of a solvated metal ion (M^{n+}) and the bulk solvent (reaction 2) has been studied for cations of many elements of the periodic table. The incoming solvent molecule S* is denoted with an asterix to distinguish it from the initially coordinated molecule with which it exchanges. Such reactions are very important in coordination chemistry and knowledge of the kinetic and associated activation parameters represents an important background for understanding the substitution of solvent by other ligands [1]. The focus has frequently, but by no means exclusively, been on water as solvent. A summary of experimental rate constants for water exchange reactions on aquated metal ions is shown in Fig. 2.

The data in Fig. 2 demonstrate that the rate constants for water exchange reactions cover almost 19 orders of magnitude, ranging from extremely slow reactions with a half-life of thousands of years to extremely fast reactions with a half-life in the nanosecond time range. Experimental water exchange rate constants are mainly determined from NMR measurements using ^{17}O-labelling techniques. The rate constants are first order or pseudo-first order and do not allow a direct mechanistic conclusion except in terms of the observed trend and that expected on the basis of the electronic structure of the metal ion. For this reason kineticists have turned to the determination of activation parameters from the temperature ($\Delta H^{\#}$ and $\Delta S^{\#}$) and pressure ($\Delta V^{\#}$) dependence of the reaction. In this respect it is important that mechanistic information is revealed by the sign and magnitude of the activation entropy ($\Delta S^{\#}$) in terms of changes in order on going to the transition state, and the value of the activation volume ($\Delta V^{\#}$) which represents changes in partial molar volume in going to the transition state. The uncertainty in the determination of $\Delta S^{\#}$ as a result of the intrinsic extrapolation to $1/T = 0$ required to determine its experimental value, has motivated kineticists to apply high pressure techniques to determine $\Delta V^{\#}$ from the pressure dependence of the water exchange rate constants. Our present understanding of the mechanism of water exchange reactions is largely based on volume of activation data determined for such processes [2]. For this purpose, much development has gone into high-pressure NMR techniques in order to enable the experimental determination of this kinetic parameter.

The advantage of the volume of activation for water exchange reactions as a mechanistic discrimination parameter is that the reaction is symmetrical with no overall reaction volume and the exchange process is assumed to involve no major solvational changes. Thus $\Delta V^{\#}$ should be a direct measure of the intrinsic volume changes that occur, such that a continuous spectrum of transition configurations can be envisaged, ranging from a very expanded, highly dissociative one (large and

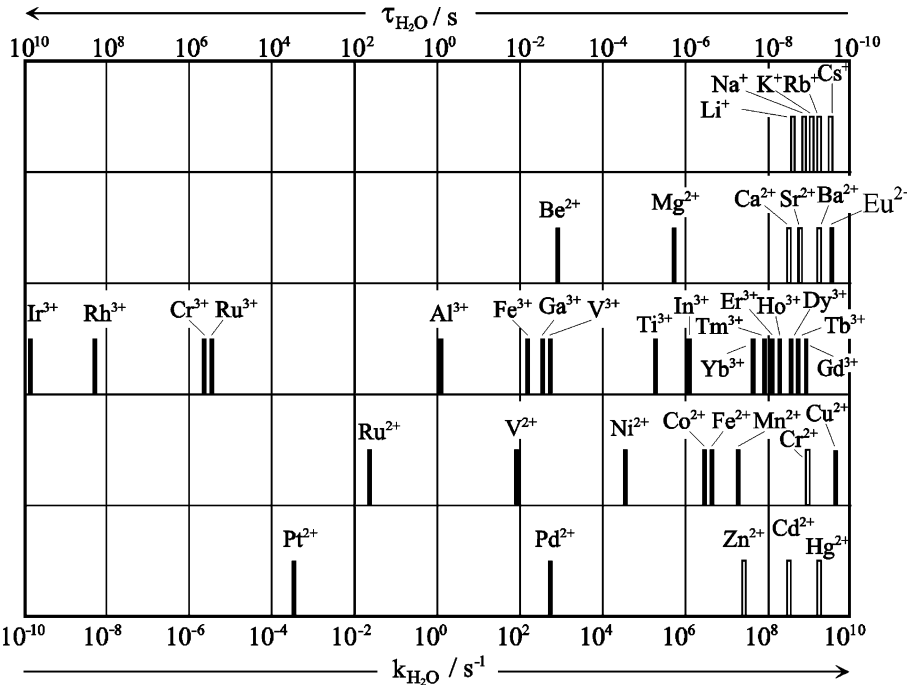

Fig. 2. Schematic representation of the lifetime of a single water molecule in the first coordination sphere, and the corresponding rate constants for water exchange reactions on aquated metal ions at 25 °C. The filled bars indicate directly determined values, and the open bars indicate values deduced from ligand substitution studies (taken from a recent review [2]).

positive $\Delta V^{\#}$; rate constant significantly slowed down by pressure) to a very compact, highly associative one (large and negative $\Delta V^{\#}$; rate constant significantly accelerated by pressure) as shown in Fig. 3.

The applications of high-pressure NMR techniques resulted in the unexpected finding of a mechanistic changeover for water exchange on divalent first row transition metal ions ($n = 2$ in equation 1) from an associative interchange (I_a) to dissociative interchange (I_d) mechanism along the series [3,4]. The $\Delta V^{\#}$ values could be accounted for in terms of bond making and bond breaking contributions as outlined for water exchange on octahedral metal ions in Fig. 4. These considerations predict a maximum volume increase (or

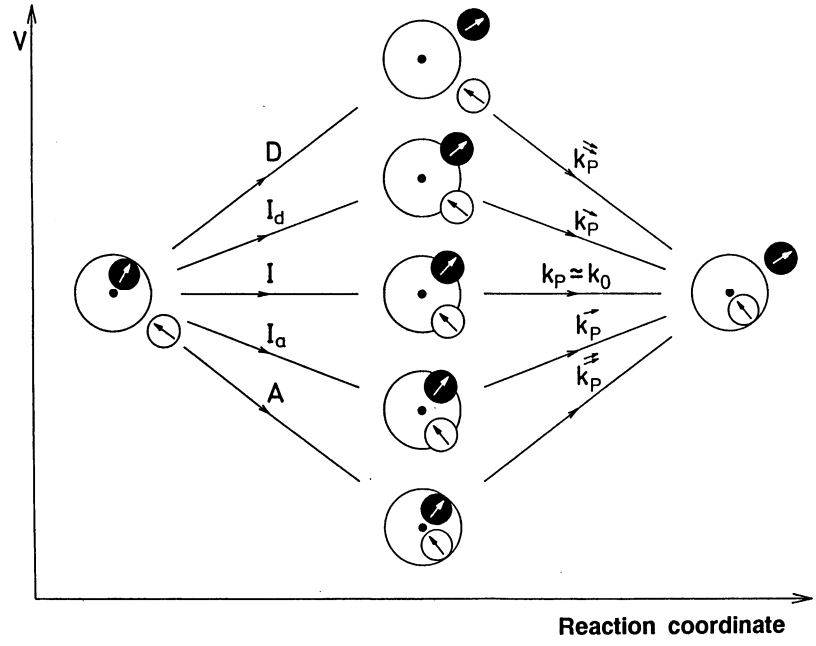

Fig. 3. Schematic volume profiles for the different solvent exchange mechanisms: k_p is the observed rate constant at a given pressure p; k_p is decelerated or accelerated on increasing pressure for a D or A mechanism, respectively [2].

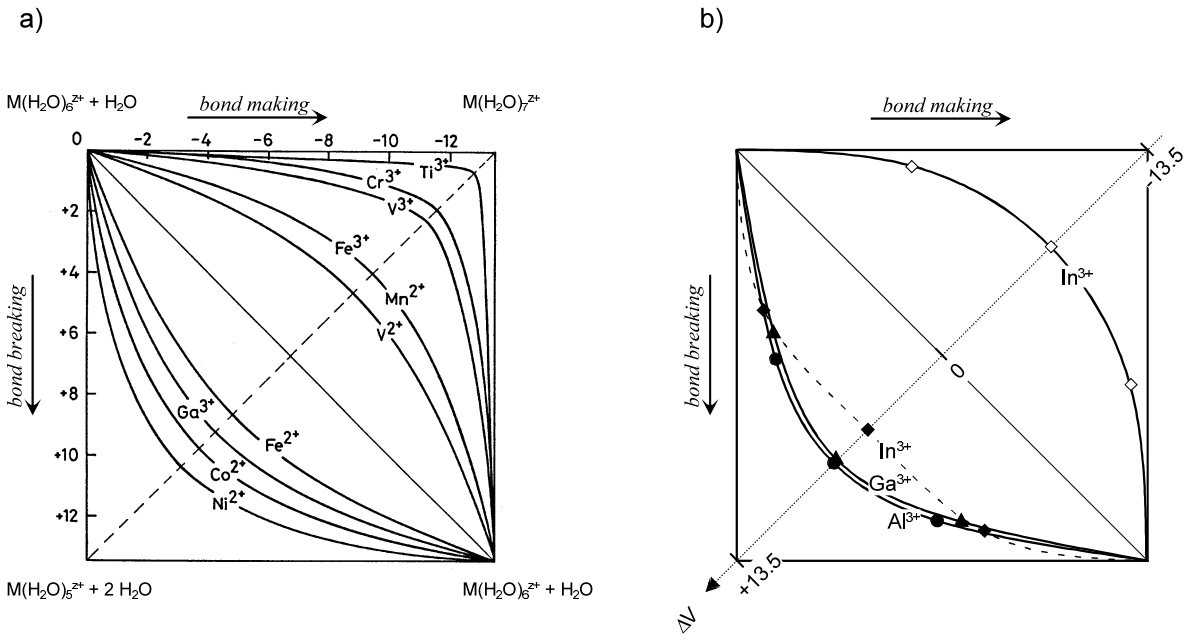

Fig. 4. Bond making and bond breaking contributions to the volumes of activation for water exchange on $[M(H_2O)_6]^{z+}$: (a) summary of volumes of activation for metal aqua ions; (b) calculated curves for Al(III), Ga(III), and In(III) with use of the Connolly volumes [6].

decrease) of 13 $cm^3\ mol^{-1}$ in the transition state for a limiting dissociative (or associative) water exchange mechanism of an octahedrally aquated metal ion. It is assumed that the bond lengths between the metal and the non-exchanging water molecules do not change significantly during the course of the reaction. The mechanistic changeover could also be seen and confirmed from studies employing other solvents and in some cases with bulky solvents, and could be understood in terms of the radius of the metal ion and electron orbital populations [5].

These mechanistic conclusions drawn from the $\Delta V^{\#}$ data were challenged on the basis of the results from theoretical calculations. A more detailed account of the apparent discrepancies between the interpretation of experimental and theoretical data will now be given.

2. Methods and theory

Theoretical studies on reaction mechanisms at metal ion centres in solution must currently use one of several approximations because of the limitations of hard- and software. As always, which approximation to use is a matter of personal preference and each of the techniques that will be described has its adherents. Basically, the problem lies in the choice between describing the bonding and electronic characteristics of the metal centre and its surroundings as well as possible or performing calculations on a system realistic enough to simulate the conditions in solution. Avogadro's number is very large and the electrostatic influence of highly charged metal ions is very far-reaching, so that realistic simulations of exchange- and other processes at metal ion centres in solution presents a formidable computational challenge. Firstly, however, we should consider the calculational methods available for determining the energy and gradients (the first derivatives of the energy with respect to geometric changes) needed for geometry optimisations, determination of normal frequencies and molecular dynamics calculations.

2.1. Force fields

Molecular mechanics, or force field, calculations represent the molecule(s) to be calculated as simple mechanical and electrostatic models. They thus by definition do not treat the system itself, but rather the model. Force fields are simply these mechanical/electrostatic models that are usually parameterised to reproduce selected properties (usually geometries and energies) of analogous molecular systems. Water models, for instance, have been parameterised to fit the known physical properties of liquid water. This means that the partial charges that determine the electrostatic behaviour of the model are appropriate for water molecules in the pure liquid phase. Such models are generally more polar than 'gas phase' water because the individual molecules in condensed water polarise each other. One very successful and often used such water model is Jorgensen's TIP4P [7]. However, the electrostatic fields encountered close to metal ions are very much larger than those found in pure water. Thus, the transferability of properties (i.e. the fact that all water

models behave in the same way) does not apply between pure water and solutions of metal salts, or even between waters close to and far away from ions in solution. Thus, standard water models cannot reproduce the cooperative effects, for instance in hydrogen-bonding, resulting from polarisation. The solution to this problem is to use polarisable force fields such as those introduced by van Duijnen [8], but these have not yet found general acceptance and most simulations reported so far have used standard water models.

2.2. Semiempirical MO-theory

Semiempirical MO-theory is usually taken to mean the modern variants of neglect of differential diatomic overlap (NDDO [9]) theory, MNDO [10], AM1 [11], or PM3 [12]. Although these methods are computationally extremely fast, they are severely limited for the study of metals [13]. The three standard methods use minimal Slater basis sets of only valence s- and p-orbitals, so that they cannot, for instance, treat any transition metals, for which valence d-orbitals are needed. Thiel et al. [14] have reported the implementation of Slater d-orbital basis sets within the NDDO-framework, but have only published parameters for a few metals. Based on this work, however, Hehre et al. [15] and Stewart [16] have produced as yet unpublished parameterisations for many transition metals. These techniques, known as PM3-tm [15] and extended AM1, PM3 and PM5 parameterisations [16] are available in commercial program packages, but have not yet undergone the rigorous scrutiny afforded for published calculational methods. Recently, however, two evaluations of the PM3-tm have been published, one favourable and one less so [17,18]. Until either the techniques are published or others become available, studies with the 'commercial' methods require very careful evaluation and testing by comparison with high level (ab initio or density functional) calculations. The published AM1 and PM3 techniques have, however, proved to be fairly reliable for the main group metals lithium [19], magnesium [20], aluminium [21], calcium [22] and zinc [20].

2.3. Ab initio molecular orbital theory

The common ab initio molecular orbital techniques that have enjoyed so much success in treating organic molecules and reactions [23] can only be applied with difficulty to transition metal systems. Frenking [24] produced a compendium of methods and calculational levels necessary to obtain reliable results for transition metal systems. In some cases, simple Hartree–Fock favours the higher coordination numbers for metal–water complexes [25]. Much better results have been obtained with post-HF methods like second order Möller–Plesset perturbation theory (MP2). However, these methods are computationally more expensive and scale with high powers of the number of basis functions (orbitals), so that they can often not be applied to experimental systems, which are typically large. Even more computationally demanding techniques such as CAS-SCF [26] are also even more reliable, but their use for water exchange reactions requires very extensive dedicated computing facilities. Nevertheless, Rotzinger [27] has used such techniques to investigate cluster models. In general practice, however, calculations on water-exchange reactions are most often performed with density functional theory (DFT), although this may not be the best choice from the theoretical point of view.

2.4. Density functional theory (DFT)

The advent of modern DFT methods for molecular systems has revolutionised computational chemistry, especially for the transition metals [28]. In a nutshell, DFT is based on the fact that all molecular electronic properties can be calculated if the electron density is known. The only blemish is that the exact form of all the components of the functional (a function of a function) that gives the energy from the electron density is unknown. There is, however, a number of approximate functionals available. These can be divided into three classes:

- Functionals based on the local density approximation (LDA) only depend on the value of the electron density at any given point in space. Such functionals are computationally very fast, but tend towards systematic errors such as overestimating bond dissociation energies and are no longer used intensively.
- Functionals that use not only the value of the electron density, but also its gradient (how fast it changes in space) are based on the generalised gradient approximation (GGA). These functionals, especially in their more modern forms, can give remarkably accurate results and are still computationally very efficient.
- Hybrid density functional techniques combine GGA functionals with a parameterised proportion of the exchange energy calculated by Hartree–Fock (HF) theory. They are thus a cross between DFT and conventional HF ab initio theory. The HF-component of the calculations requires that the two-electron integrals necessary for conventional HF-calculations be determined, which make hybrid methods significantly slower than 'pure' DFT techniques. However, hybrid DFT methods are the most accurate of the three classes and, therefore, enjoy great popularity. The best-known hybrid level of theory is Becke's three-parameter technique with the Lee–Yang–Parr correlation functional (B3LYP) [29]. However, recent studies on the relative energies of different spin states

of transition metal complexes [30] suggest that the standard B3LYP technique may not be the best possible for these systems.

The two major advantages of DFT calculations in the context of this review are that they give good to excellent results for metal systems, including transition metals, and that they scale relatively well with the size of the system to be calculated, so that large complexes and clusters can be treated. However, DFT shows some serious limitations for studying water-exchange reactions. Hydrogen-bonding and proton-transfer reactions are generally not treated well by DFT [31,32]. Compared with MP2, even hybrid DFT with an adequate basis set also favours lower coordination numbers [33]. Additionally, DFT gives inaccurate geometries for 3+ first row transition metals. This is especially true for systems in which more than one coordination sphere is considered [33]. Thus, the good agreement often found between experiment and DFT results may sometimes be fortuitous. The development of appropriate functionals is a very active research area and could eliminate these limitations.

The above methods, however, only provide us with a means to calculate the structures, energies, normal vibrations and electronic characteristics of the systems of interest. How can they be used to study processes occurring at metal ion centres in solution? Ideally, we would like to calculate the dynamics of a system of a macroscopic amount of water at the best possible calculational level for a time long enough for us to observe the reactions of interest and to obtain statistically reliable thermodynamics. Consider, however, that even a picomole of water contains 6×10^{11} atoms, compared with the largest simulations performed to date of about 10^7 atoms with a highly simplified force field. Assuming a time step of 1 fs for molecular dynamics calculations, we would need 10^6 energy and gradient evaluations for a 1 ns simulation. Now consider that one energy/gradient evaluation for a hexaaqua metal ion system (19 atoms) using B3LYP with a good basis set requires about 1 h of CPU time on a modern processor and you can visualise the magnitude of the problem.

Clearly, we must make approximations in the system to be calculated, not only in the calculational methods themselves. The following sections describe the possibilities.

2.5. Cluster calculations

Cluster calculations are performed on model clusters that usually consist of the metal ion and its first coordination sphere, sometimes also the first solvation sphere. These clusters may or may not be a good approximation to the real situation of the metal ion in solution. The very few available comparisons suggest that clusters are generally a good approximation. They have the advantage that minima and transition states can be optimised and characterised in order to study reactions. Their major disadvantage is that, if the coordination number is not known, it must be determined by adding extra solvent molecules to the first coordination sphere or the first solvation sphere in order to test which is the more stable. Even then, there is no guarantee that the correct coordination number for an ion in solution can be determined. It might seem that the larger the cluster calculation, the better the approximation to a real solution, but this is not necessarily the case. The more atoms that are included in a system, the larger the number of degrees of freedom and the higher the number of likely minimum energy structures. At some point the number of possible minima becomes so large that is no longer sensible to speak of a single minimum energy structure. The real system is dynamic and would 'visit' many energetically similar structures during any experimental observation that we might make. There is, however, an alternative that can be used to make cluster calculations more realistic. We can use a polarisable continuum to simulate the time-averaged water molecules that surround the cluster in solution.

2.6. Continuum models of solvation

There are two main types of continuum solvation models, the polarisable continuum model (PCM) pioneered by Tomasi and his group [34] and the conductor-like shielding model (COSMO) introduced by Klamt and Schüürmann [35]. In both cases the molecule is surrounded by virtual charges that polarise it as a surrounding solvent would. These charges are situated on the surface of an imaginary cavity in the solvent. In the PCM-techniques, the magnitude of the virtual charges is calculated as though the molecule were surrounded by a polarisable continuum of the appropriate dielectric constant using the Kirkwood method [36] or by solving the Laplace–Poisson equations with the proper boundary conditions. The virtual charges can also interact with each other on the cavity surface, resulting in a so-called self-polarisation correction. COSMO treats the solvent as a conductor, so that the cavity acts as a Faraday cage. COSMO is thus often called a perfect shielding model. One of the major problems is to define the imaginary cavity in the solvent. There are many different variations available for PCM calculations, but COSMO usually uses the incomplete van der Waals' cavity introduced by Klamt and Schüürman [35].

Both models can give good results. Their major weakness is that they cannot reproduce specific interactions with the surrounding solvent, such as long-lived

hydrogen bonds. Thus, the boundary between the cluster (the 'supermolecule') and the continuum should be in a region where specific long-lived hydrogen bonds are not found.

2.7. Molecular dynamics and Monte Carlo

The solution to the problem of multiple minima in realistic model systems for solvation is to use a technique that either simulates the movements of the individual atoms and molecules over time (molecular dynamics (MD) [37]) or uses random moves combined with a statistical stability test to establish thermal equilibrium (Monte Carlo calculations (MC) [38]). Generally, MC calculations are preferable for all problems in which only thermodynamic equilibrium conformations of the system are of interest, including free energy perturbation calculations [39], whereas MD calculations are used when a real time scale is needed, as in kinetic investigations of all types. We will concentrate on MD simulations here because they have been used far more frequently than MC for the area of interest.

2.7.1. Classical MD

By far the largest number of simulations of solvated metal ions has been performed using classical (force field) MD simulations. The results must be treated with some circumspection because of the general use of non-polarisable force fields, which may not reproduce the bonding characteristics around the metal ion at all well. A further concern with classical simulations is the reliability of the force field parameters for the metal ions, which may not be based on a large enough amount of data. However, classical MD simulations generally treat very large systems in comparison to other types of calculation and are, therefore, the most reliable from this point of view. The simulations usually use periodic boundary conditions, which mean that a 'box' containing the system to be simulated is surrounded by identical boxes on all sides. Thus, if a water molecule leaves its box on one side, it reappears at the opposite side. This technique allows the simulation of effectively very large systems, but is limited by the possibility that ions in adjacent boxes may interact with each other significantly and thus falsify the results (see below).

2.7.2. Direct semiempirical MO–MD

A technique that has recently been used to study hydration of metal ions is direct semiempirical MO–MD. 'Direct' means that the energies and gradients required for the MD calculation are obtained directly from semiempirical MO calculations. This technique has the major advantage that polarisation of the solvent molecules by the metal ion is included in the calculations automatically. It is, however, significantly slower than classical MD and can, therefore, only be applied to relatively small systems (100–150 water molecules) and for short simulation times. At present, periodic boundary conditions are not used, but rather the system is confined to a sphere of the correct volume by a harmonic constraining potential. This technique avoids the problem of electrostatic images of neighbouring boxes but may introduce spurious mechanical forces into the simulation.

2.7.3. Carr–Parinello MD (CPMD)

Carr–Parinello MD is a special variation of DFT used for dynamics calculations. The 'trick' is to treat the electronic degrees of freedom of the system (in this case the electron density) as fictitious degrees of freedom in the MD calculation. In this way it is no longer necessary to converge the electron density at every time step as is the case in direct MO–MD or would be the case in direct DFT–MD. The resulting technique is computationally very efficient (for a DFT method) and lends itself well to efficient implementation on parallel computers. CPMD is, however, still very much more CPU-intensive than semiempirical MO–MD and is, therefore, usually limited to smaller systems and requires very much more expensive hardware. CPMD simulations use periodic boundary conditions, which seriously limits their effectiveness for the problems considered here. Consider a typical system consisting of one metal ion and 50 water molecules. The concentration of metal ions in the periodically reproduced system is 1 mol of metal ions per 50 mol (900 g) of water, which is 1.1 M. Thus, the simulations actually treat a 1.1 M solution of metal ions without counter ions. Put another way, the edge dimensions of a cubic box of 50 water molecules are 11.4 Å at a density of 1.0 g ml^{-1}. The metal ions in adjacent boxes are thus 11.4 Å apart. The Coulombic interaction energy between two dipositive ions at this distance assuming a constant dielectric of 78.36 (water) is 5.9 kJ mol^{-1} and the electrostatic field due to the ion at the centres of the faces of the box is roughly 100 MV m^{-1}. Thus, all MD simulations using periodic boundary conditions need to use a very large water box in order to avoid strong electrostatic interference between neighbouring box images. However, simulations of this size are currently not possible, so that all conclusions drawn from periodic boundary MD simulations (CPMD, direct MO or classical) with small water boxes must be treated with caution. Note, however, that Car–Parinello simulations use only non-hybrid DFT-functionals and so all the limitations outlined in Section 2.4 for static DFT also apply in this case.

2.7.4. Other techniques

A number of other techniques are possible for simulating hydrated metal ions. At first sight, quantum mechanical MD simulations with a surrounding continuum model solvent seem attractive. However, the

continuum does not provide the specific hydrogen bonding to the boundary waters, which thus tend to spin around their principal axes in simulations because this movement is not hindered by the solvent continuum. Perhaps the most promising techniques are those involving a combination of quantum mechanics for the central part of the simulation, which is then surrounded by a classical (force field) solvent. Such so-called quantum mechanical/molecular mechanical (QM/MM) techniques are now well established for studies of enzyme reaction mechanisms using either semiempirical MO-theory [40], or either normal DFT [41] or Carr–Parinello DFT [42] for the quantum mechanical part. A further promising approach is the use of frozen orbitals to represent distant solvent molecules in DFT calculations [43]. Such techniques are very promising for simulations of solvated metal ions.

3. Results

3.1. Water exchange in the first coordination sphere

We will first consider water exchange reactions on fully hydrated metal ions, which in terms of the coordination chemistry involved represent the simplest case. Subsequently, we will focus on water exchange reactions in the presence of spectator ligands that can labilise the metal ion and so affect the water exchange mechanism.

3.1.1. Pure aqua complexes

On the basis of a simplified gas-phase cluster approach, the water exchange mechanisms of di- and trivalent metal ions have been calculated successfully with ab initio and DFT methods over the past years. In these reactions, where the reactant and the product species are identical, the reactivity (lability) of the metal centre tunes the rate and mechanism of the exchange reaction. Depending on the metal and its charge, the observed water exchange rate covers more then 18 orders of magnitude as shown in Fig. 2. That means a mean lifetime of a water molecule in the first coordination sphere from 200 ps (Cs^+) up to 300 years and more (Ir^{3+}) [44]. Helm and Merbach recently summarised some general trends for water exchange reactions based on experimental (NMR) $\Delta V^{\#}$ values and theoretical calculations [45]. The computational treatment of these reactions is based on the mechanistic models for A, D and $I_{a/d}$ mechanisms mentioned before with particular attention for the starting structures, because of the still inhomogeneous picture for such fundamental properties as the number of solvent molecules in the first and/or higher coordination spheres or the geometry of the complexes. In the case of Cu(II) a DFT study of $[Cu(H_2O)_n]^{2+}$ with $n = 3$–8 found for $n = 8$ the most stable structure with four inner shell water molecules and the other four doubly-hydrogen-bonded to the water molecules of the first shell [46]. In other studies five- and six-fold coordination was found to be preferred [47,48]. A detailed investigation of the different symmetries (Fig. 5) of the first row transition metal hexaaqua complexes was recently reported by Kallies et al. [49]. They used density-functional calculations combined with the natural localised bond orbital method to analyse the individual contributions coming from the metal ion's 3d σ-, 3d π-, and 4s σ-interactions.

The unexpected finding of a mechanistic changeover for water exchange on divalent first row transition metal ions ($n = 2$ in reaction 1) from an associative interchange (I_a) to dissociative interchange (I_d) mechanism along the series [50,51], caught the attention of theoreticians. On the basis of calculations, it was claimed that the mechanism of solvent exchange is I_d throughout the divalent first row transition metal series [52–54]. Later calculations showed that the experimentalists' analysis was correct [25,27]. These included ab initio calculations at the self consistent field (SCF), Hartree–Fock or complete active space-(CAS)-SCF levels. It was now possible to generate A, I_a, I_d, and D pathways, and to optimise the structures of the transition and intermediate states. Different metal–water clusters that can occur along the reaction coordinate of a water exchange process must be calculated. A comparison of energies and structural parameters like metal–oxygen bond distances in the reactants, transition states and intermediates will help to associate them with different reaction mechanisms. All pertinent transition states and intermediates that could occur along the reaction coordinate of an associative, a concerted interchange, and a dissociative water exchange process were calculated successfully with these methods. In addition, Merbach, Rotzinger and co-workers have revised the interpretation of the water exchange reactions of Al(III), Ga(III), and In(III) using new experimental data in conjunction with ab initio calculations of approximate gas-phase metal–aqua clusters [6]. By comparison of experimental and theoretical results the authors clearly showed that the use of such gas-phase models, which only account for a complete first coordination sphere, is justified in order to reproduce the water exchange reactions of metal ions in solution.

The transition states shown in Figs. 6 and 7 demonstrate the A character for water exchange on Ti^{3+}, the I_a character for water exchange on V^{2+}, and the D or I_d character for water exchange on Ni^{2+}, respectively. DFT has also been used successfully to describe water exchange on Zn^{2+} [55] and Ti^{3+} [56]. A review of experimental and theoretical aspects of water exchange on metal ions appeared recently [2]. It should be kept in mind that these calculations are limited to the gas phase ($T = 0$ K), i.e. the role of the second coordination (first

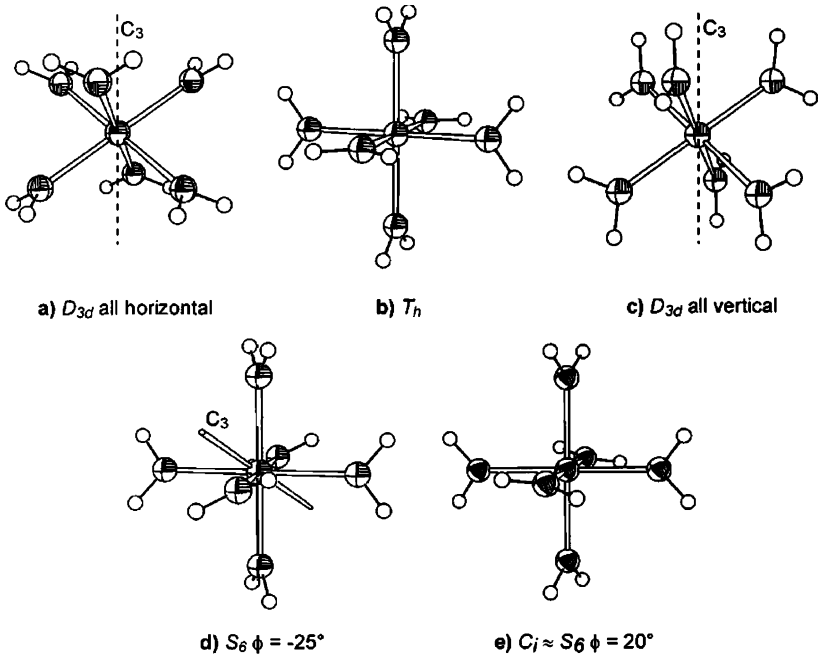

Fig. 5. Conformations studied for $[Ti(H_2O)_6]^{3+}$ and $[V(H_2O)_6]^{3+}$ with planarly ligating water molecules [49].

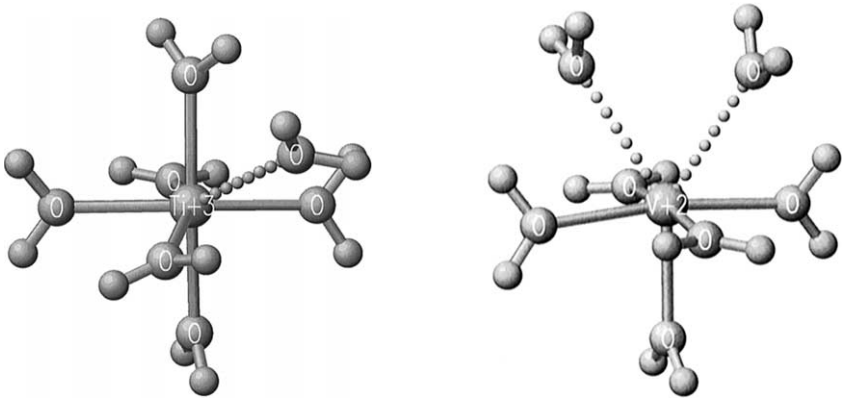

Fig. 6. Optimised transition states calculated for water exchange on Ti^{3+} and V^{2+} [27].

solvation) sphere or the influence of counter ions is not explicitly taken into account.

We will now, by way of examples, discuss DFT calculations on the water exchange on the octahedral Ti^{3+} and Zn^{2+} and the square-planar Pd and Pt complexes. For Zn^{2+} a dissociative D mechanism was found, in good agreement with experimental data and HF calculations. The choice of exchange mechanism is based on the computed activation energy, the geometry of the identified transition states and intermediates, and the sum of all M–O distances in the stationary structures during the reaction. The latter can be used as an approximation to the experimentally important activation volume ($\Delta V^{\#}$) values. The structures and hydration energies were computed for $[Zn(H_2O)_n]^{2+}$ with $n = 1$–6 and for $[Zn(H_2O)_n]^{2+} \cdot mH_2O$ with $n = 5$ and $m = 1,2$, and $n = 6$ and $m = 1$. The $[Zn(H_2O)_n]^{2+}$ structure could be shown to be the more favourable compared with the $[Zn(H_2O)_5]^{2+} \cdot H_2O$ coordination

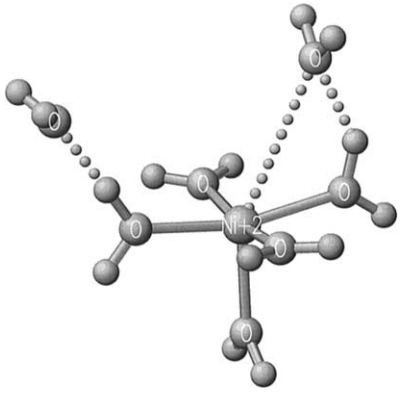

Fig. 7. Optimised transition states calculated for water exchange on Ni^{2+} [27].

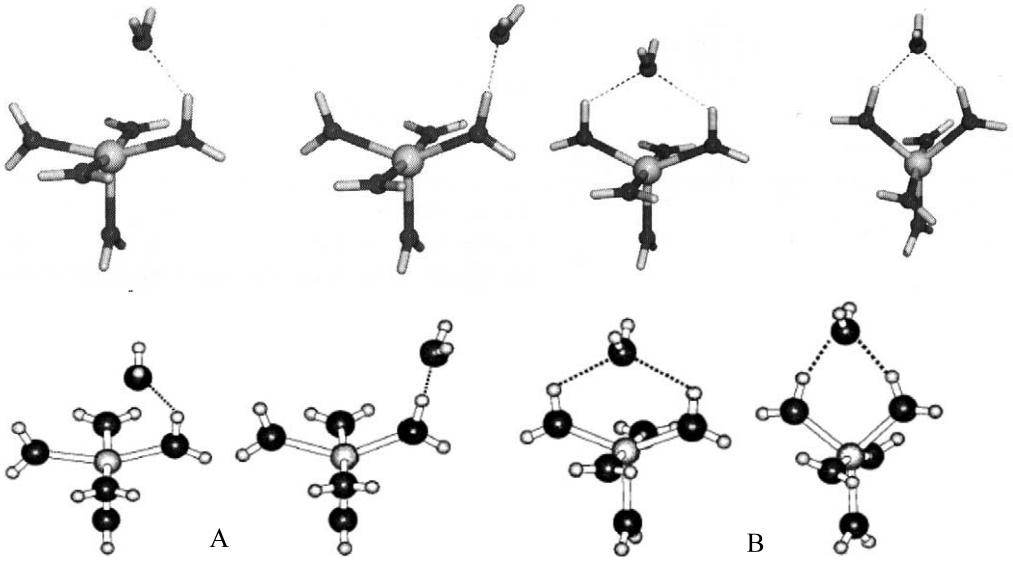

Fig. 8. Transition state and intermediate complexes for $[Zn(H_2O)_n]^{2+}$ with one (A) or two (B) hydrogen bonds between first and second sphere water molecules [55].

[57]. There are two types of complexes with water molecules in the second coordination sphere having either one or two hydrogen bonds between the first and second sphere water molecules as shown in Fig. 8.

The energy of activation for the dissociative water exchange on $[Zn(H_2O)_6]^{2+}$ with two hydrogen bonds to the first sphere averages 17.6 kJ mol^{-1} with Zn–O distances for the leaving water of the reactant to the transition and intermediate state of 2.13, 2.83 and 3.85 Å, respectively. For the single hydrogen bond path these values are 2.13, 3.06 and 4.10 Å. The structures found for this reaction are very similar to those found by Rotzinger for Ni^{2+} [27]. Considering more than six water molecules, that means one or more water molecules of the second coordination sphere, e.g. the reaction $[Zn(H_2O)_6]^{2+} \cdot H_2O \rightarrow [Zn(H_2O)_5]^{2+} \cdot 2H_2O$, leads to a negative ΔE and, therefore, favours a penta-coordinate Zn^{2+}, in contrast to MP2 results [33].

Other examples, however, for the successful application of DFT for water exchange reactions are the associative water exchange reactions found for aqueous Ti^{3+}, Pd^{2+} and Pt^{2+} [50,58]. In the Ti^{3+} case, the energy of activation was calculated to be 66.1 kJ mol^{-1}, which is too high compared with the experimental value of 43.1 kJ mol^{-1} [59], but the mechanistic conclusions arising from these calculations, namely the preferred associative reaction mechanism, agree well with experimental data. In addition, on trying to simulate the dissociative pathway for the water exchange on Ti^{3+}, a strong tendency for a proton transfer from a coordinated to the leaving water molecule was found. Calculations for the water exchange of the corresponding hydroxo–aqua complexes $[Ti(H_2O)_5(OH)]^{2+}$ and $[Ti(H_2O)_5(OH)]^{2+} \cdot H_2O$ were found to proceed via limiting D mechanisms with energies of activation of 38.5 and 30.1 kJ mol^{-1}, respectively. This implies a complete changeover from A to D as the preferred pathway for water exchange on the hexaaqua and pentaaquahydroxo complex ions, which can be expected on the basis of the available experimental data for water exchange on other trivalent ions [60–64]. In general, the exchange rate for these metal ions is enhanced by a factor of 10^2–10^3 by the labilising effects of coordinated OH^-, in particular for the water molecule *trans* to the hydroxo ligand, and correlates with a changeover in water exchange mechanism. This pK_a dependence could be confirmed theoretically. A detailed study of the influence of the hydroxo ligand on geometric and electronic properties for main group and first row transition metal ions has been reported [65].

The results of DFT calculations using the LDA for the square-planar $[Pd/Pt(H_2O)_4]^{2+}$ complexes, strongly suggest an associative water exchange mechanism. Both, the structures of the tetra-aqua complexes and the energies of activation for the exchange reactions of these complexes, viz. 57 and 92 kJ mol^{-1} for Pd and Pt, respectively, are in good agreement with available experimental data, viz. 50 and 90 kJ mol^{-1}, respectively. The best results have been obtained by considering relativistic effects explicitly on all Pt structures. It could be shown that DFT with a relativistic correction for heavy atoms gives very good results for the total molecular energies, while absolute reproduction of the observed $\Delta H^{\neq}$ values for the water exchange on $[Pd(H_2O)_4]^{2+}$ and $[Pt(H_2O)_4]^{2+}$ complexes requires an explicit energy correction for solvation. We will return to this point later.

3.1.2. Influence of spectator ligands

Various groups have performed theoretical studies concerning the influence of spectator ligands on the water exchange mechanism. Rotzinger et al. studied the water exchange reaction on $[Ru(NH_3)_5OH_2]^{3+}$, $[Rh(NH_3)_5OH_2]^{3+}$ and $[Rh(NH_2CH_3)_5OH_2]^{3+}$ by ab initio CAS-SCF and MCQDPT2 calculations [66,67]. Water-exchange on $[Rh(NH_3)_5OH_2]^{3+}$ most likely proceeds via the I (interchange) mechanism, whereas that on $[Rh(NH_2CH_3)_5OH_2]^{3+}$ follows a dissociative (I_d or D) pathway caused by the bulky NH_2CH_3 ligands. Both reactions proceed with retention of configuration. For the ammonia complex, the computed activation energy agrees with experiment, whereas for the methylamine complex the equal activation energies for both the I_d and the D pathways are 22 kJ mol^{-1} lower than $\Delta H^{\#}_{298}$. On the basis of this result the distinction between the two mechanisms is not possible and an extended model system with explicit considered water molecules in the second sphere is necessary. The more associative character found for the water exchange on $[Ru(NH_3)_5OH_2]^{3+}$, I_a, versus I for $[Rh(NH_3)_5OH_2]^{3+}$, results from the fact that the antibonding d_β orbitals are occupied by one less electron, which, therefore, gives a shorter metal–oxygen distance in the transition state. The activation volumes for both amine complexes are known to be equal, but since $\Delta\Sigma\, d$(Ru–L) is more negative than $\Delta\Sigma\, d$(Rh–L), $\Delta V^{\#}_{int}$ for Ru(III) is also expected to be more negative than $\Delta V^{\#}_{int}$ for Rh(III) and, therefore, $\Delta V^{\#}_{el}$ must be more positive for Ru(III) than for Rh(III).

In a further study, Rotzinger obtained very similar results for the exchange mechanisms of various Cr^{3+} complexes [68]. The bulky ligands in $[Cr(NH_2CH_3)_5OH_2]^{3+}$ result in a dissociative water exchange mechanism, whereas all other complexes studied from $[Cr(NH_3)_5OH_2]^{3+}$, *trans*-$[Cr(NH_3)_4(OH_2)_2]^{3+}$, *trans*-$[Cr\text{-}(NH_3)_4(NH_2CH_3)OH_2]^{3+}$ to the pure $[Ru(OH_2)_6]^{3+}$ and $[Cr(OH_2)_6]^{3+}$ complexes exchange via an I_a mechanism, again with retention of the configuration. The metal–oxygen distances in the transition states correlate with the basicity of the ligands, and the effect of the *trans* ligand is larger than that of the *cis*.

The mechanisms for water exchange between $[UO_2(H_2O)_5]^{2+}$ and $[UO_2(oxalate)_2(H_2O)]^{2-}$, and solvent water along dissociative (D), associative (A) and interchange (I) pathways were studied by Grenthe et al. [69] using HF/MP2. The geometries of the A- and I-transition states for both $[UO_2(H_2O)_5]^{2+}$ and $[UO_2(oxalate)_2(H_2O)]^{2-}$ indicates that the entering/leaving water molecules are located outside the plane formed by the spectator ligands (Figs. 9 and 10).

These quantities were calculated both in the gas phase and within the PCM for the solvent. There is a significant and predictable difference between the activation energy in the gas phase and the solvent models: the energy barrier for the reaction via the D mechanism increases in the solvent as compared with the gas phase, whereas it decreases for the modelled A and I_a mechanisms. The calculated activation energy for water exchange on $[UO_2(H_2O)_5]^{2+}$ was found to be 19 and 21 kJ mol^{-1} for the A and I_a mechanisms, respectively, as compared with the experimental $\Delta H^{\neq} = 26 \pm 1$ kJ mol^{-1}. Because of the low energy barrier between transition state and intermediate, it is very difficult to distinguish which mechanism actually operates. In contrast, the activation energy for water exchange on the $[UO_2(oxalate)_2(H_2O)]^{2-}$ complex following D, A and I mechanisms, is 56, 12 and 53 kJ mol^{-1}, respectively. This indicates that in this case the water exchange follows an associative reaction mechanism, which is unexpected if neutral ligands are replaced by anions. However, the U=O bonds found in this study are consistently 0.1 Å too short and the U–OH_2 bonds are too long. This effect may change the calculated reaction mechanism. A better agreement at least for the U=O bond lengths can be achieved using DFT with relativistic core potentials [70].

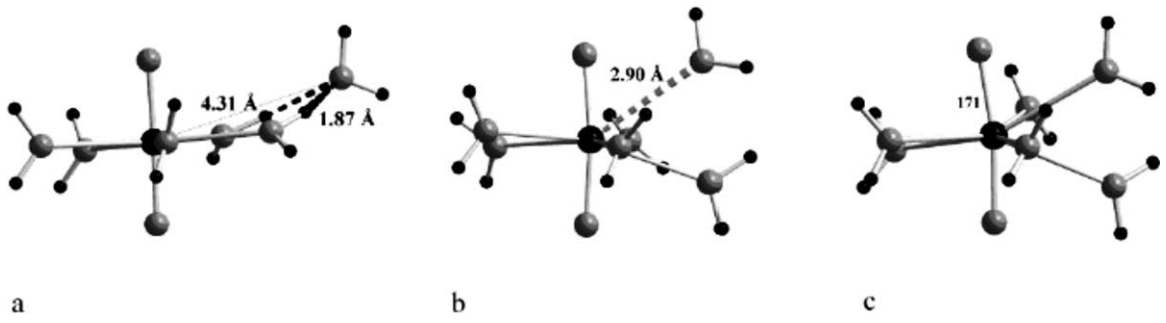

Fig. 9. The A-mechanism for the uranyl(VI)–aqua ion. Perspective views of the reactant $[UO_2(H_2O)_5]^{2+} \cdot (H_2O)$ (a), transition state $\{[UO_2(H_2O)_5 \cdots (H_2O)]^{2+}\}^{\neq}$ (b), and the six-coordinate intermediate $[UO_2(H_2O)_6]^{2+}$ (c). The uranium atom and the hydrogen atoms are black and the oxygen atoms medium grey. The thin lines denote the distance between non-bonded atoms, and the dark dashed lines hydrogen-bond interactions. The light dashed bond denotes the leaving water in the transition state [69].

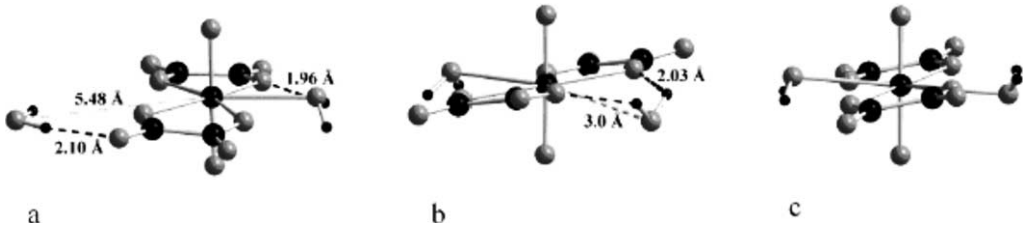

Fig. 10. The A-mechanism for the uranyl(VI)–oxalate complex. Perspective views of the reactant $[UO_2(C_2O_4)_2(H_2O)]^{2-}\cdot(H_2O)$ (a), transition state $\{[UO_2(C_2O_4)_2(H_2O)\cdots(H_2O)]^{2-}\}^{\neq}$ (b), and six-coordinate intermediate $[UO_2(C_2O_4)_2(H_2O)_2]^{2-}$ (c) [69].

3.2. Water exchange between first and second coordination sphere

Computational studies of aquated metal complexes with explicit quantum-mechanical consideration of the second coordination sphere, are quite rare. In such model systems, the aquated metal ions should consist of four to six or more water molecules in the first coordination sphere and up to 12 further water molecules in the second coordination sphere (first solvation sphere), which are fully taken into account in the water exchange reaction [71]. The transition state for water exchange will then involve solvent molecules from both the first and second coordination (solvation) spheres. Due to the large number of conformations and the *flat energy hypersurface* found for such systems, even the calculation of possible ground states requires much computational effort. Another difficulty, as mentioned above, is the description of the coordination sphere of aqueous metal ions, which can differ depending on the method used. An example can be found in the work of Merz et al., who investigated the first and second coordination sphere of hydrated Zn^{2+} with HF, MP2 and DFT methods [33]. They found that HF and DFT predict $[Zn(H_2O)_4](H_2O)_8^{2+}$ to be more stable than $[Zn(H_2O)_6](H_2O)_6^{2+}$. The experimentally known preferred six-fold coordination could only be reproduced with MP2. Aqueous iron and manganese complexes

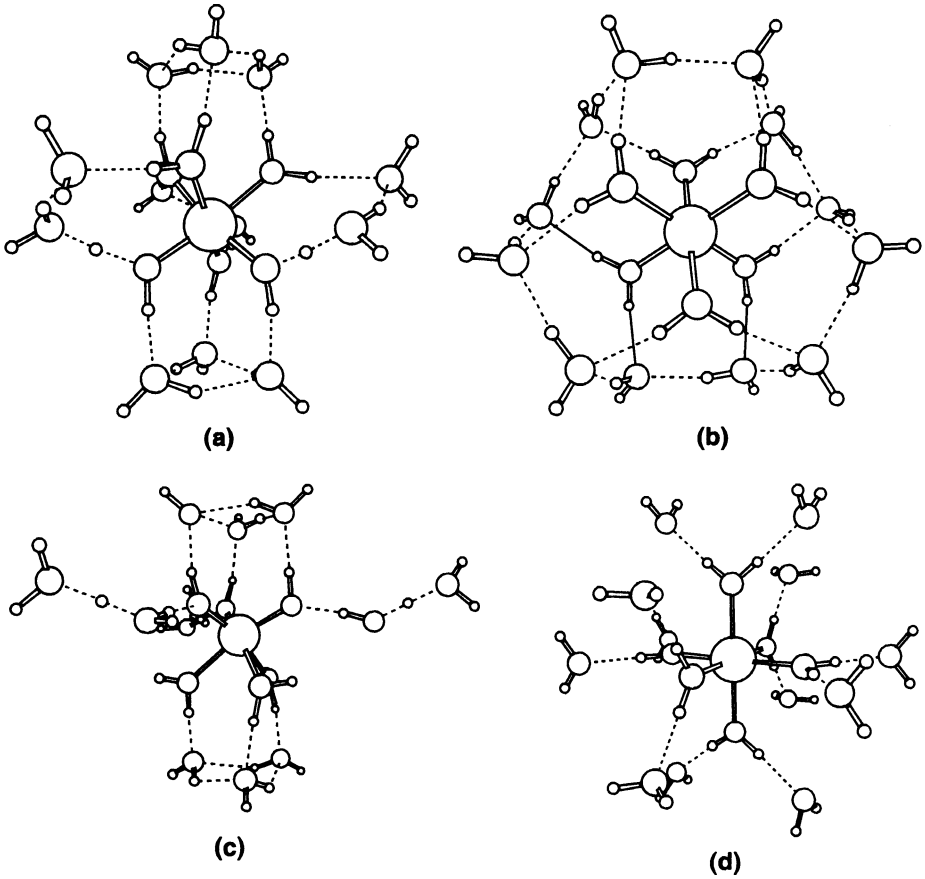

Fig. 11. (a) and (b) The two types of Ti(+2, +3, +4) with 18 water molecules structures; (c) Proton transfer in type (a) structure found for Ti^{4+}; (d) T_h structure used by Li [72] (for titanium as central ion this structure represents a higher-order saddle point) [73].

were studied by Li et al. [72]. Tamm et al. [73] applied DFT to titanium complexes containing six or 18 water molecules. They considered charges of +2, +3 and +4 for the titanium ion, as well as different geometries for the hexaaqua complexes used as starting structures to construct the second coordination sphere. Inclusion of the second coordination sphere led to two geometrically distinct types of minima for the titanium cations, viz. (a) and (b) in Fig. 11. For the Ti^{4+} ion, the relatively flat structure was found to be of lowest energy. In this close to C_3 structure, five distinct groups, two of them containing three and three of them containing two water molecules, are found. In addition, a transfer of three protons to the outermost water molecules took place in this structure, (c) in Fig. 11, which corresponds to the known hydrolysis of Ti^{4+} in water. In contrast, for the Ti^{2+} and Ti^{3+} central ions, the more spherically distributed structure, characterised by two nine-molecules sets of hydrogen-bonded waters in two parallel planes, was found as lowest energy structure. No proton transfer was reported for these complexes. The effect on the Ti–O distances in the first coordination sphere depends on the charge on the metal ion. All Ti–O bond lengths are shortened by 2–4 pm, except for Ti^{4+}, where the bonds are elongated by 2.17–2.19 pm.

In these studies mainly the coordination geometries were investigated. At present, no such large calculations on water exchange reactions have been reported. Clearly, much more theoretical work will be required to be able to treat such more realistic model systems.

3.3. Continuum solvation models

Many models have been developed over the years to describe the molecular interaction in solution. A detailed overview of the work done in this area can by found in the reviews by Tomasi [34,74], Rivail and Rinaldi [75], Cramer and Truhlar [76], Richards [77], and as the most current one, Cramer and Truhlar [78]. In general, the studies in the field of solvation continuum for aqua complexes concern two main areas. First, and this includes the majority of papers, implementation and validation of the models are performed. Second, some work on water exchange reactions has been published. For all this studies it should be kept in mind that continuum solvation models are limited to describing the time-average of the solute–solvent effects.

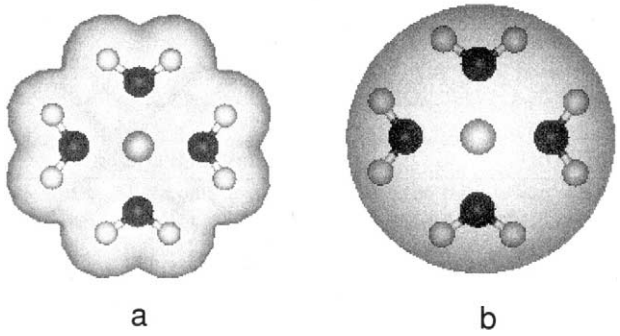

Fig. 12. Cavity shape used in the PCM model (a) and the Nancy's MPE model (b) for the Be^{2+} tetrahydrate [82].

Within the PCM, the solvent is represented by a homogeneous dielectric continuum, which is polarised by the charge distribution of the solute and polarises the solute itself in a self-consistent way. In the standard PCM the solute is placed within a cavity in the dielectric, defined in terms of interlocking spheres centred on the solute's nuclear positions (see Fig. 12a). During geometry optimisations the cavity boundaries follow the changes in the nuclear positions [79,80]. It is also possible to use PCM with a fixed cavity of a given shape, e.g. a sphere. In both cases the solute–solvent interactions are described in terms of a solvent reaction potential, which is defined by a set of surface charges located on the cavity surface. The problem is then shifted to the definition of the proper apparent surface charge. In practice, the cavity surface is divided into small triangles called 'tesserae'. Induced charges are placed at the centre of each triangle in order to simulate the reaction field. In this scheme, the reaction potential introduced in the effective Hamiltonian is reduced to one-electron operators depending on the surface charges.

In another widely used model, the reaction field multipole expansion method (MPE), the solute's charge distribution is defined by means of a multipole expansion centred on a representative point of the cavity [81] (monocentric expansion). The use of a constant coordinate cavity (like a sphere or an ellipsoid, see Fig. 12b), enables an analytical expression for the multipole moments which simplifies the quantum chemical implementation of the method. The solvent reaction field is defined as the linear response of the dielectric medium to the multipole expansion of the solute charge distribution, weighted by a function of the dielectric permittivity and the cavity properties, called 'reaction field factor'. The solute–solvent interaction is defined as the generalised product of the solvent reaction field and molecular multipole moments.

The influence of these two solvation models on the metal–oxygen distance of a set of hydrated cations $[M(H_2O)_m]^{n+}$, where $M = Be^{2+}$, Mg^{2+}, Ca^{2+}, Zn^{2+}, and Al^{3+}, with respect to that found for the hydrated metal in vacuum, was studied by Tomasi et al. [82]. Within the continuum solvation model, they compared the MPE [81], using a spherical cavity, and the PCM [34] in its recent re-formulation [83,84], using a molecularly shaped cavity (Fig. 12). Opposite tendencies, a shortening or a lengthening of the metal–oxygen distance, are known for these models. In this study the substantial

equivalence of the two methods when the spherical cavity is used, was demonstrated. For the most interesting parameter, viz. the metal–oxygen distance, an increase of 0.013–0.064 Å was found for these complexes. On the other hand, a better agreement to discrete solvation models, where a small number of solvent molecules is explicitly considered [85,86], is observed when the PCM method with a cavity fitting the molecular shape is used. The average effect is similar to the results of Rudolph et al. for Al^{3+}, Mg^{2+} and Zn^{2+} [87–89], who found a decrease in d_{M-O} between 0.015 and 0.025 Å, and to the work of Pavlov et al. for the divalent cations using a discrete second shell [90]. A mixed discrete and continuum solvation model was used by Marcos et al. for the hydration of Ag(I) [91]. They found opposite effects on the Ag–O distance for the two models. The interactions of the discrete solvation formed by two water shells (4+8) shortens the Ag–O distance, mainly by hydrogen bonding, whereas the long-range interactions caused by the continuum lengthen the bonds. This can lead to a mutual cancellation of the effects when the two solvation models are used jointly. As mentioned above, the construction of the solute cavities plays an important role and therein the atomic radii. A parameterisation of the atomic radii for the whole Ln(III) series was performed by Cosentino et al. [92]. With their optimised radii, they reached agreement with experimental values on molecular structures, relative stability of the octa- with respect to the nona-hydrated species, and hydration free energies for the neodymium(III) and ytterbium(III) aqueous ions studied. Earlier DFT calculations within the PCM model for the redox potentials and absolute pK_a values of transition metal ions in solution [93] gave good results for the potentials, but significant differences for the pK_a values.

A mechanistic study of water exchange on $[V(H_2O)_6]^{2+}$, $[Mn(H_2O)_6]^{2+}$ and $[Fe(H_2O)_6]^{2+}$, including electron correlation and the influence of the solvent, was reported by Rotzinger [94]. In this work, ab initio HF calculations combined with the PCM model for the solvent were used. The two reaction paths for the water exchange process as illustrated in Fig. 8 for the $[M(H_2O)_6]^{2+} \cdot H_2O$ adducts, viz. associative (I_a or A) and dissociative (D) mechanisms, were investigated. Activation energies in agreement with experimental data were obtained for water exchange on V^{2+}, Mn^{2+} and Fe^{2+} via the bridging bound way. Experimental and theoretical results suggest A and D activation for $[V(H_2O)_6]^{2+}$ and $[Fe(H_2O)_6]^{2+}$, respectively, whereas for $[Mn(H_2O)_6]^{2+}$ the activation energies for the A and D mechanisms are equal. Therefore, it is not possible to distinguish between the two mechanisms with this model.

4. Dynamic methods

The methods described above give very accurate structures and energies for the computed systems. The quality of these calculations is mainly limited by the necessary computational efforts to solve the integrals required by the theoretical model. However, even the highest level of calculations discussed until now, only allow static pictures of the processes occurring in the system. Furthermore, they are limited to a small number of solvent molecules, usually the first coordination sphere. To overcome these gas phase limitations and to include higher coordination spheres, dynamic methods are widely used. They vary from classical MD for very large systems, i.e. thousands of solvent molecules, to high-level Car–Parrinello simulations for a comparatively small solvent box which consider all included solvent molecules explicitly. Thus the solute–solvent interaction, and in particular H-bonding between the first and second coordination spheres, are considered quantum mechanically. These methods can provide realistic insight into the time-dependent behaviour of a system. Unfortunately, they are either computationally very expensive or simplifications must be made that limit the accuracy expected. For the MM simulations, the potential energy models are simply based on the summation of the interactions between pairs of particles, thus neglecting higher order terms. A full QM treatment of such a system requires enormous computational effort, but allows much more accurate interaction potentials, calculated from the instantaneous configurations including many-body effects. Due to the computational effort, either specifically constructed force fields, for example for the chloro ions of platinum group complexes [95], or a hybrid approach such as QM/MM are widely used.

4.1. Classical MD and mixed QM/MM

Extensive MD and MC calculations using three- and lower-body potentials based on ab initio calculations of triplets of water [96–99] have shown that the static properties of water, such as the structure as demonstrated by the radial distribution functions, do not change as much as dynamic properties when three-body potentials are applied [100]. In the case of multivalent metal cations in water, MD studies using pair potentials fitted by ab initio energies have given apparently incorrect results because of the non-additivity of the interaction potentials, i.e. in the neglect of the many-body forces. Including the three-body terms, results in a four-fold coordination structure of Be^{2+} [101], which is the experimentally known value, versus the $[Be(H_2O)_6]^{2+}$ structure found when these terms are neglected. Similar results were obtained for Li^+ [102] and Ni^{2+}. For the latter a coordination sphere contain-

ing more then six water molecules was found [103]. Detailed studies on the two- and higher-order interaction energy terms for Al^{3+} in the $[Al(H_2O)_6]^{3+}$ cluster complete the situation [104]. The three-body interactions were found to be one third the size of the sum of the two-body interactions and are opposite in sign. The four- and higher-body contributions on the interaction energy are much smaller. Recent dynamic studies show the influence of such terms for an aqueous $AlCl_3$ solution, which led to a closer agreement with experimental results, e.g. for the vibrational spectra [105].

The Cu^{2+} hydration shell structure has been studied by a combination of ab initio QM/MM Monte Carlo simulation by Rode et al. [47], using both the classical pair and the three-body potentials for the bulk water. Their system consists of one Cu^{2+} ion and 399 water molecules in the periodic cube at a temperature of 298.16 K and a density of 0.997 g cm^{-1}. The QM/MM simulation results in two distinctly separated hydration shells at a distance of 2.08 and 3.3–4.9 Å, which are more compact and shifted to shorter distances than those of the MM simulation, where the first shell peak is centred at 2.20 Å and the second shell covers the range from 3.0 to 5.3 Å. The most prominent changes occur in the second hydration shell, which appears less diffuse in the QM/MM than in the MM case. The mean coordination number for the first shell amounts to 6 and for the second shell to 14.5, in contrast to 18.3 in the classical case (Fig. 13). The experimental values for the second sphere range from 7.6 to 11.6 at a distance of 4.1–4.2 Å [106–108].

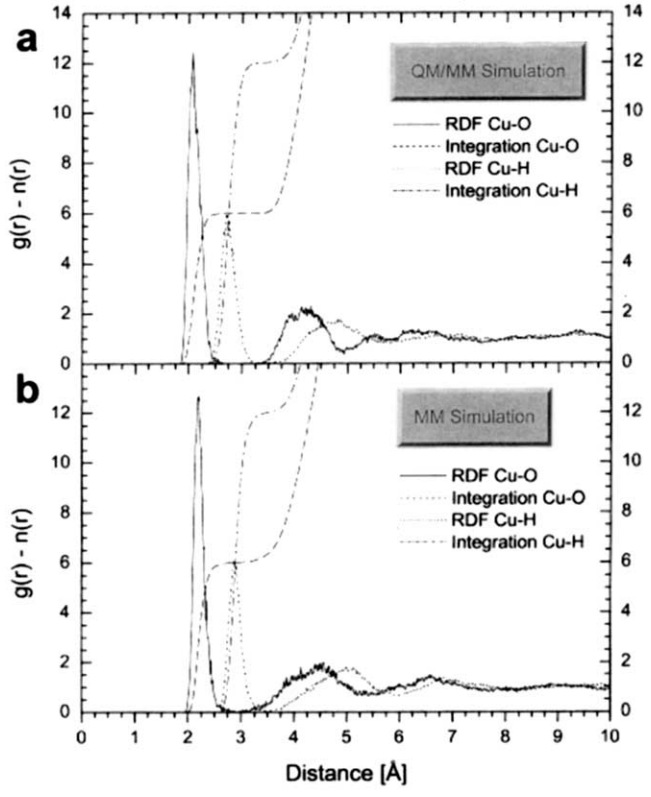

Fig. 13. Coordination number distributions of the hydrated Cu(II), comparing first and second shell for the QM/MM and the MM simulation [47].

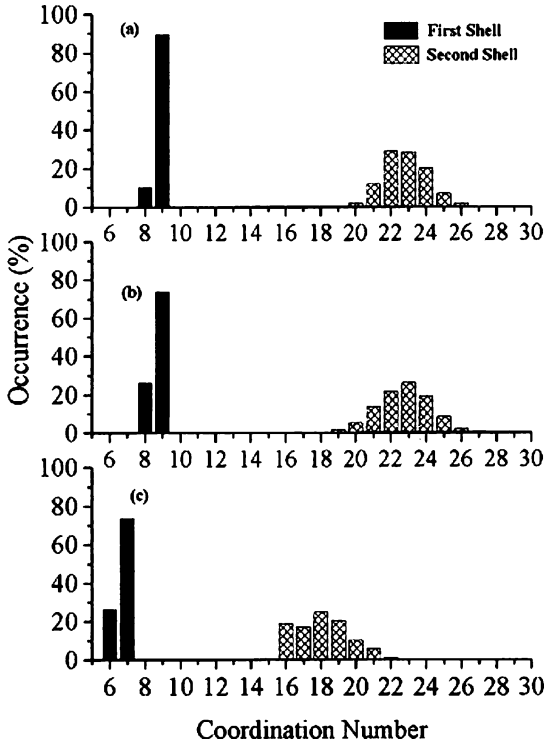

Fig. 14. First- and second-shell coordination number distribution of hydrated Mn(II) for the (a) MC, (b) MD, and (c) QM/MM–MD simulations [109].

The same authors obtained similar results for aqueous Mn^{2+} (Fig. 14) [109]. For the MC simulation, coordination numbers of 10.33% of eight and 89.67% of nine, with a mean value of 8.90 water molecules, and for the MD simulation, 26% of eight, 73.73% of nine and 0.27% of ten water molecules, with a mean value of 8.74 water molecules, were observed. However, for the QM/MM–MD simulation, 26.42% of six and 73.57% of seven water molecules around the cation with a mean value of 6.74 water molecules were obtained, i.e. about two water molecules less than the averages obtained from the classical MC/MD simulations. The mean coordination numbers for the second hydration shell are 22.83, 22.74, and 18.06 for MC, MD, and QM/MM–MD simulations, respectively, implying that every first shell water molecule interacts with about 2.6 water molecules in the second shell. Again, the results of the QM/MM–MD methodology are much closer to the experimental values.

Yang et al. reported QM/MM simulations on thorium(IV) hydrates in aqueous solution [110]. The hydration of the Th^{4+} ion in an aqueous system was first investigated using B3LYP hybrid DFT calculations. The

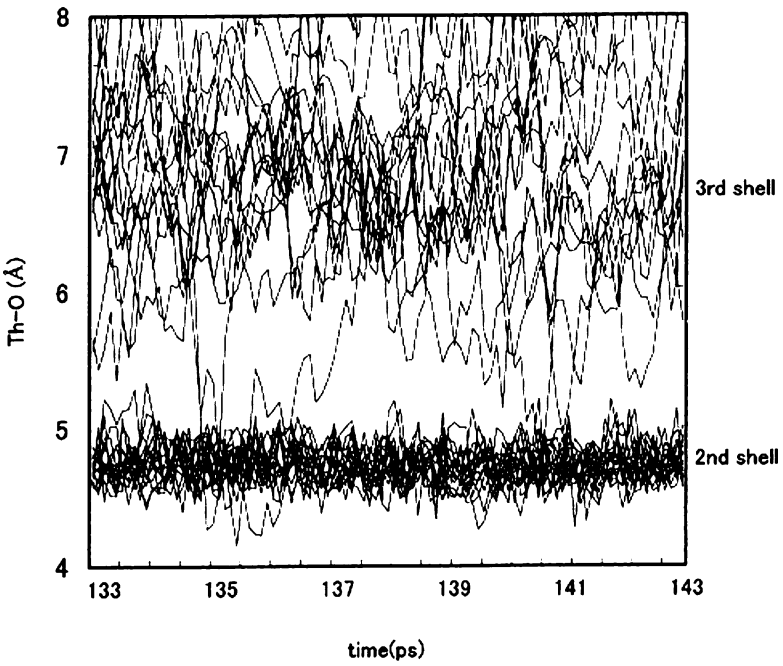

Fig. 15. Thorium–oxygen distance for a 10 ps interval showing the water exchange between the second hydration shell and the bulk [110].

first shell hydration number of Th^{4+} ion in the liquid phase was found to be 9 (C_{4v} geometry) at bond distances of Th–O(I) 2.54(1) Å and Th–H(I) 3.22(1) Å. However, the ten-coordinate structure is calculated to be within 0.7 kcal mol^{-1}, so that no definite conclusion about the coordination number can be drawn in this case. The second shell hydration properties were studied by MD simulation using the AMBER force field. The concept of the hydrated ion [111] as reported and validated by Martinez et al. [112] and Bleuzen et al. [113] was used, $[Th(H_2O)_9]^{4+}$ being the cationic entity interacting in solution. The $[Th(H_2O)_9]^{4+}$–water interaction potential was developed by B3LYP calculations. The partial atomic charge of $[Th(H_2O)_9]^{4+}$ was derived from the ESP method. The MD calculated results show a well-defined second coordination shell and an ill-defined third shell around the $[Th(H_2O)_9]^{4+}$ ion. Strong hydrogen bonding due to polarisation of the first coordination sphere water molecules leads to a mean coordination number of 18.9 water molecules in the second shell at bond distances of Th–O(II) 4.75 Å and Th–H(II) 5.35 Å. The residence time of a water molecule in the second hydration shell is 423.4 ps. A plot of all Th–O distances during the simulation is shown in Fig. 15.

Schwenk et al. studied the dynamics of the solvation process and water exchange between the first and second coordination sphere of Ca^{2+} in water in a similar way [114]. Their QM part was treated with the canonical HF method on the one hand and with DFT on the other hand. In both simulations, one water exchange took place during a simulation time of 10 ps. In the QM/MM–HF simulation the time required for an exchange was 2.0 ps, and in the QM/MM–DFT simulation 1.2 ps. Both simulations started with a stable eight-fold coordination but differed in the exchange mechanism. During the DFT simulation an additional water molecule entered the first coordination sphere, stayed there for 1.2 ps and then the same molecule left again (Fig. 16). In contrast, during the HF simulation, one water molecule left the first coordination sphere and entered again after 2 ps as shown in Fig. 17. The systems contained one Ca^{2+} ion and 199 water molecules in a periodic cube. For the QM region the diameter was 8.0 Å with a smoothing function for the transition between the QM and the MM part. Further details are given in the literature [114]. In an earlier study the same authors [115] compared classical, HF and DFT simulations with regard to the first coordination sphere on the aqueous Ca^{2+} system. The first shell contains an average of 7.1 (classical), 7.6 (HF) and 8.1 (DFT) water molecules, respectively, whereas the second shell consists of 17.9, 19.1 and 20.5 water molecules, respectively, during the simulations.

Such simulations are not limited to aqueous systems but can also be performed for other solvents like ammonia [116,117], or mixed aqueous ammonia solutions [118]. Another field where MD simulations have been applied successfully, is chelate complexes including water molecules. For these systems the dissociation of the bound water is of main interest. Some poly(aminocarboxylate)gadolinium(III) type complexes, widely used as magnetic resonance imaging (MRI) contrast agents, have been studied with dynamic methods [119].

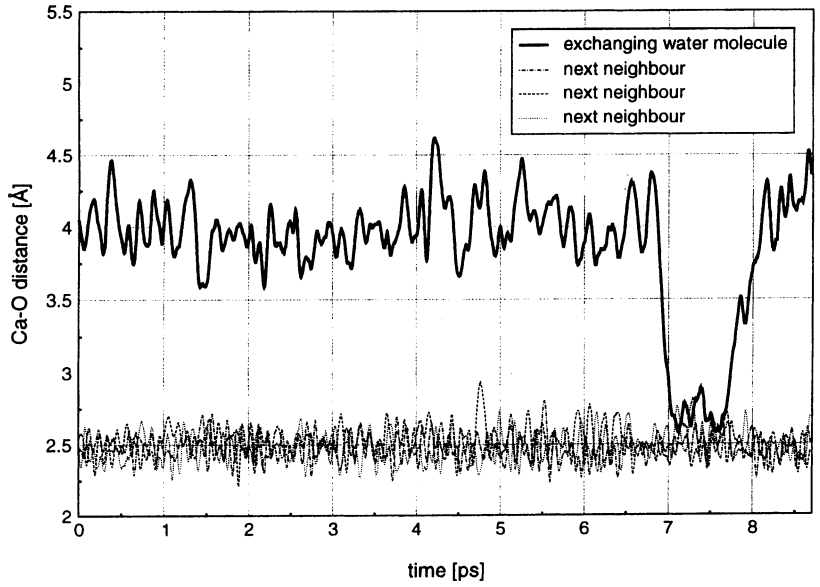

Fig. 16. Variation of the Ca–O distances of the exchanging water molecule and of its nearest three neighbouring water molecules during the DFT/MM simulation, showing a change of the coordination number from 8 to 9 and back [114].

In a recent MD study by Yerley et al. [120] using two different X-ray structures as starting point, the volume of activation for the water dissociation on $[Gd(egta)(H_2O)]^-$ could be calculated from the simulation data to be $+7.2$ cm^3 mol^{-1}, in acceptable agreement to the experimental value of $+10.5$ cm^3 mol^{-1}. Very fast conformational changes of the chelate complex related to the electronic relaxation of the complex have been observed independently to the dissociation of water.

4.2. Car–Parrinello MD

Few examples for first-principles molecular dynamics studies are available in the literature. Marx et al. [121] applied the Car–Parrinello method to describe the Be^{2+} cation and 32 water molecules for a total simulation time of 1 ps. A recent study on the first solvation shell of the Cu^{2+} aqua ion using the Car–Parrinello method was performed by Merbach et al. [48]. The structure of the hydrated Cu^{2+} complex was determined by neutron

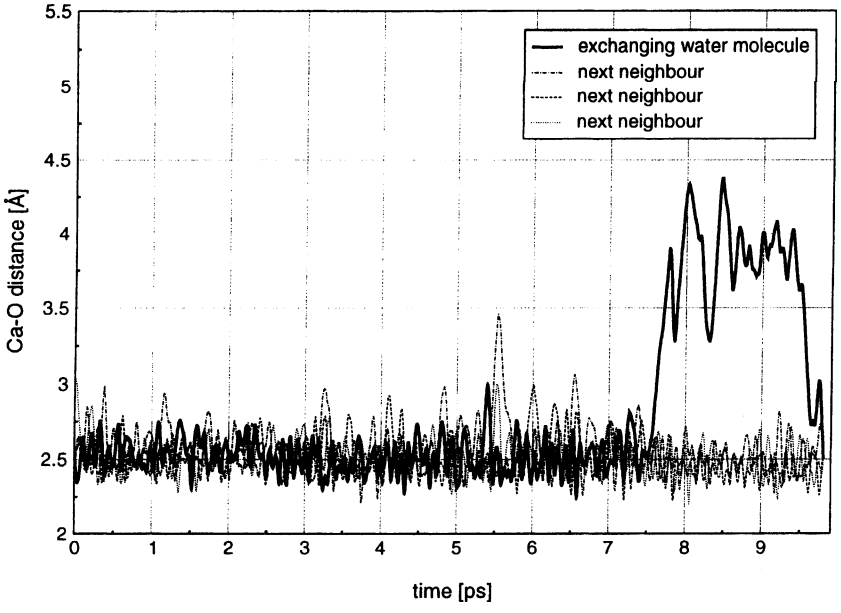

Fig. 17. Variation of the Ca–O distances of the exchanging water molecule and of its nearest three neighbouring water molecules during the HF/MM simulation, showing a change of the coordination number from 8 to 7 and back [114].

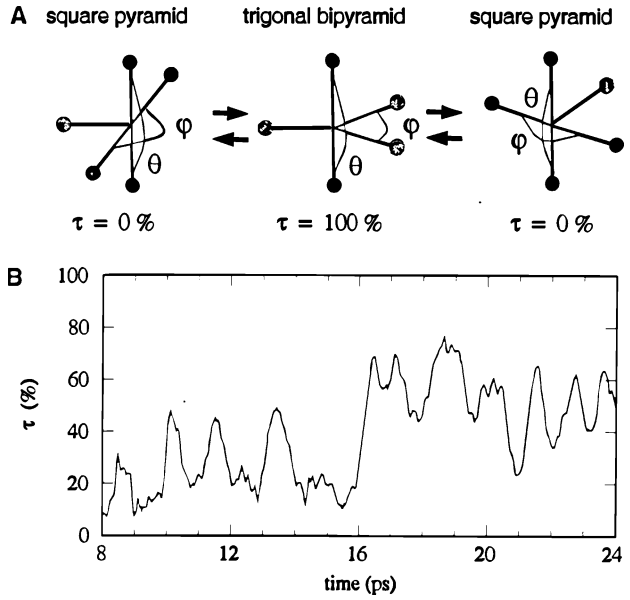

Fig. 18. (A) Berry twist mechanism showing, from left to right, the reorientation of the main axis of a square pyramidal configuration by pseudorotations via a trigonal bipyramidal configuration (θ, φ are O–Cu–O angles, $\tau = (\theta - \varphi)/60 \times 100\%$). (B) Evolution of τ as derived from the Car–Parrinello simulation (window-averaged over an interval of 0.5 ps). The parameter τ describes intermediate configurations of the five-coordinate Cu(II) aqua ion ranging between the regular square pyramidal ($\tau = 0\%$) and the regular bipyramidal ($\tau = 100\%$) configurations [48].

diffraction and first-principles molecular dynamics [122–124]. Both the experimental and theoretical results provide evidence for a five-fold coordination of the Cu^{2+} ion, in contrast to the generally accepted distorted octahedral coordination. The simulations used a periodically repeated system consisting of a single Cu^{2+} ion and 50 water molecules. After a testing and equilibrium phase, data was collected at 350 K for 17 ps. For 16 ps of this simulation the Cu^{2+} was five-fold coordinated. The authors performed several tests of the theoretical approach. They repeated the simulation under the same conditions with Ni^{2+} instead of Cu^{2+}, which resulted in the expected six-fold coordination of Ni^{2+}. Using a selected structure from this simulation and replacing Ni^{2+} by Cu^{2+}, the five-fold coordination was recovered. This behaviour can be explained by a Jahn–Teller destabilisation of the octahedral configuration for Cu^{2+} as a consequence of the $3d^9$ electronic state and was observed as a frequent transformation between square pyramidal and trigonal bipyramidal configurations (Berry twist) during the simulation, as shown in Fig. 18.

Note, however, that all the limitations of both DFT in general (Section 2.4) and of limited size CPMD simulations (Section 3.7.3) apply to these calculations, so that the results are by no means universally accepted. Persson et al. [125], for instance, have recently reported experimental evidence from an EXAFS study that copper(II) ions are six-coordinate in aqueous solution. Their results are not consistent with those of the CPMD study. The development of appropriate functionals, especially for H-bonding, can help to overcome these limitations.

5. Conclusions

Water exchange reactions on transition metal ions play a fundamental role in all biological and environmental processes in aqueous medium in which the lability of metal ions and complexes control the efficiency of the overall process. The mechanistic insight gained over the past two to three decades mainly relies on volume of activation data for such reactions which present an intrinsic picture of volume changes associated with the water exchange process. Theoretical descriptions of such reactions on aquated metal ions at a molecular level in the gas phase, have up to now confirmed the mechanistic formulations derived on the basis of volume of activation data. However, these theoretical descriptions are still far away from the real chemical system consisting of aquated metal ions in solution, in which a distinction between the first coordination sphere, the second coordination (first solvation) sphere and the bulk solvent is made. Some progress (as described in this review) has been made in considering the first and second coordination spheres in theoretical calculations on water exchange processes, but the size of such systems has slowed down the expected progress. Once it is possible to describe water exchange processes between the first and second coordination spheres more accurately, it is our belief that we will be rather close to the description of systems in the liquid phase where the water exchange process is mainly controlled by these two spheres. The alternative approach to adopt molecular dynamics to describe the interaction between a metal ion and a large number of water molecules in a defined space (box) has revealed some interesting results, but a real mechanistic understanding of water exchange processes and the nature of the transition state based on such data remains an object for the future. Nevertheless, the ability to analyse existing experimental data and to predict data for systems that have not been or cannot be studied experimentally, has developed impressively over the past few years. In this respect, it is reasonable to expect significant progress in the theoretical description of water, solvent and ligand exchange processes in future as improved hardware and software packages become available.

Acknowledgements

The authors gratefully acknowledge financial support from the Deutsche Forschungsgemeinschaft within SFB 583 on 'Redox active metal complexes—Controlling reactivity through molecular architectures'. The authors appreciate the thorough and valuable comments made by a reviewer.

References

[1] J. Burgess, Metal Ions in Solution, Ellis Horwood, Chichester, 1978.
[2] L. Helm, A.E. Merbach, Coord. Chem. Rev. 187 (1999) 151.
[3] Y. Ducommun, K.E. Newman, A.E. Merbach, Inorg. Chem. 19 (1980) 3696.
[4] Y. Ducommun, D. Zbinden, A. Merbach, Helv. Chim. Acta 65 (1982) 1385.
[5] (a) L. Fielding, P. Moore, J. Chem. Soc. Chem. Commun. 49 (1988);
(b) L. Fielding, P. Moore, J. Chem. Soc. Dalton Trans. 873 (1989).
[6] T. Kowall, P. Caravan, H. Bourgeois, L. Helm, F.P. Rotzinger, A.E. Merbach, J. Am. Chem. Soc. 120 (1998) 6569.
[7] W.L. Jorgensen, J. Chandrasekhar, J.D. Madura, R.W. Impey, M.L. Klein, J. Chem. Phys. 79 (1983) 926.
[8] J.A.C. Rullmann, P.T. van Duijnen, Mol. Phys. 63 (1988) 451.
[9] J.A. Pople, D.P. Santry, G.A. Segal, J. Chem. Phys. 43 (1965) 129.
[10] (a) M.J.S. Dewar, W. Thiel, J. Am. Chem. Soc. 99 (1997) 4899, 4907;
(b) MNDO, W. Thiel, in: P.V.R. Schleyer, N.L. Allinger, T. Clark, J. Gasteiger, P.A. Kollman, H.F. Schaefer, III, P.R. Schreiner (eds.), Encyclopedia of Computational Chemistry, Wiley, Chichester, vol. 3, 1998, p. 1599.
[11] (a) M.J.S. Dewar, E.G. Zoebisch, E.F. Healy, J.J.P. Stewart, J. Am. Chem. Soc. 107 (1985) 3902;
(b) AM1, A.J. Holder, P.V.R. Schleyer, N.L. Allinger, T. Clark, J. Gasteiger, P.A. Kollman, H.F. Schaefer, III, P.R. Schreiner (eds.), Encyclopedia of Computational Chemistry, Wiley, Chichester, vol. 1, 1998, p. 8.
[12] (a) J.J.P. Stewart, J. Comput. Chem. 10 (1989) 209;
(b) PM3, J.J.P. Stewart, P.V.R. Schleyer, N.L. Allinger, T. Clark, J. Gasteiger, P.A. Kollman, H.F. Schaefer, III, P.R. Schreiner (eds.), Encyclopedia of Computational Chemistry, Wiley, Chichester, vol. 3, 1998, p. 2080.
[13] T. Clark, J. Mol. Struct. (Theochem.) 530 (2000) 1.
[14] (a) W. Thiel, A.A. Voityuk, Theor. Chim. Acta 81 (1992) 391;
(b) W. Thiel, A.A. Voityuk, Theor. Chim. Acta 93 (1996) 315;
(c) W. Thiel, A.A. Voityuk, Int. J. Quant. Chem. 44 (1994) 807;
(d) W. Thiel, A.A. Voityuk, J. Mol. Struct. 313 (1994) 141;
(e) W. Thiel, A.A. Voityuk, J. Phys. Chem. 100 (1996) 616;
(f) MNDO/d, W. Thiel, P.V.R. Schleyer, N.L. Allinger, T. Clark, J. Gasteiger, P.A. Kollman, H.F. Schaefer, III, P.R. Schreiner (eds.), Encyclopedia of Computational Chemistry, Wiley, Chichester, vol. 3, 1998, p. 1604.
[15] W.J. Hehre, J. Yu, Book of Abstracts, 210th ACS National Meeting, Chicago, IL, 20–24 August, 1995, (Pt. 1).
[16] http://www.cachesoftware.com/mopac/index.shtml.
[17] K.J. Børve, V.R. Jensen, T. Karlsen, J.A. Støvneng, O. Swang, J. Mol. Model. 3 (1997) 193.
[18] K.R. Adam, I.A. Atkinson, L.F. Lindoy, J. Mol. Struct. 384 (1996) 183.
[19] E. Anders, R. Koch, P. Freunscht, J. Comput. Chem. 14 (1993) 1301.
[20] J.J.P. Stewart, J. Comput. Chem. 12 (1991) 320.
[21] J.J.P. Stewart, J. Comput. Chem. 10 (1989) 209.
[22] J. Yu, W.J. Hehre, Wavefunction Inc., Irvine, CA, 1995.
[23] W.J. Hehre, L. Radom, J.A. Pople, P.V.R. Schleyer, Ab initio Molecular Orbital Theory, Wiley, New York, 1986.
[24] G. Frenking, N. Froehlich, Chem. Rev. 100 (2000) 717.
[25] F.P. Rotzinger, J. Am. Chem. Soc. 119 (1997) 5230.
[26] D. Hegarty, M.A. Robb, Mol. Phys. 38 (1979) 1795.
[27] F.P. Rotzinger, J. Am. Chem. Soc. 118 (1996) 6760.
[28] W. Koch, M.C. Holthausen, A Chemist's Guide to Density Functional Theory, 2nd ed, Wiley-VCH, Weinheim, 2001.
[29] (a) A.D. Becke, J. Chem. Phys. 98 (1993) 5648;
(b) C. Lee, W. Yang, R.G. Parr, Phys. Rev. B 37 (1988) 785.
[30] M. Reiher, O. Salomon, B.A. Hess, Theor. Chem. Accounts 107 (2001) 1.
[31] S. Shadhukhan, D. Munoz, C. Adamo, G.E. Scuseria, Chem. Phys. Lett. 306 (1999) 83.
[32] M. Pavese, S. Chawla, D. Lu, J. Lobaugh, G.A. Voth, J. Chem. Phys. 107 (1997) 7428.
[33] N. Diaz, D. Suarez, K.M. Merz, Jr., Chem. Phys. Lett. 326 (2000) 288.
[34] J. Tomasi, M. Persico, Chem. Rev. 94 (1994) 2027.
[35] A. Klamt, G. Schüürmann, J. Chem. Soc. Perkin Trans. 2 (1993) 799.
[36] J. Kirkwood, J. Chem. Phys. 2 (1934) 351.
[37] A. Rahman, F.H. Stillinger, J. Chem. Phys. 55 (1971) 3336.
[38] W.L. Jorgensen, Book of Abstracts, 212th ACS National Meeting, Orlando, FL, 1996.
[39] W.L. Jorgensen, Acc. Chem. Res. 22 (1989) 184.
[40] G. Schuerer, H. Lanig, T. Clark, J. Phys. Chem. B 104 (2000) 1349.
[41] M.R.A. Blomberg, P.E.M. Siegbahn, J. Phys. Chem. B 105 (2001) 9375.
[42] U. Röthlisberger, Comp. Chem. 6 (2001) 33.
[43] T. Wesolowski, R.P. Muller, A. Warshel, J. Phys. Chem. 100 (1996) 15444.
[44] A. Cusanelli, U. Frey, D.T. Richens, A.E. Merbach, J. Am. Chem. Soc. 118 (1996) 5265.
[45] L. Helm, A.E. Merbach, J. Chem. Soc. Dalton Trans. (2002) 633.
[46] A. Berces, T. Nukada, P. Margl, T. Ziegler, J. Phys. Chem. A 103 (1999) 9693.
[47] G.W. Marini, K.R. Liedl, B.M. Rhode, J. Phys. Chem. A 103 (1999) 11387.
[48] A. Pasquarello, I. Petri, P.S. Salmon, O. Parisel, R. Car, É. Tóth, D.H. Powell, H.E. Fischer, L. Helm, A.E. Merbach, Science 291 (2001) 856.
[49] B. Kallies, R. Meier, Inorg. Chem. 40 (2001) 3101.
[50] Y. Ducommun, K.E. Newman, A.E. Merbach, Inorg. Chem. 19 (1980) 3696.
[51] Y. Ducommun, D. Zbinden, A.E. Merbach, Helv. Chim. Acta 65 (1982) 1385.
[52] S.K. Kang, B. Lam, T.A. Albright, J.F. O'Brian, New J. Chem. 15 (1991) 757.
[53] R. Åkesson, L.G.M. Peterson, M. Sandström, P.E.M. Siegbahn, U. Wahlgren, J. Phys. Chem. 97 (1993) 3765.
[54] (a) R. Åkesson, L.G.M. Peterson, M. Sandström, U. Wahlgren, J. Am. Chem. Soc. 116 (1994) 8691;
(b) R. Åkesson, L.G.M. Peterson, M. Sandström, U. Wahlgren, J. Am. Chem. Soc. 116 (1994) 8705.
[55] M. Hartmann, T. Clark, R. van Eldik, J. Am. Chem. Soc. 119 (1997) 5867.
[56] M. Hartmann, T. Clark, R. van Eldik, J. Phys. Chem. A 103 (1999) 9899.

[57] G. Tiraboschi, N. Gresh, C. Giessner-Prettre, L.G. Pedersen, D.W. Deerfield, J. Comp. Chem. 21 (2000) 1011.
[58] R.J. Deeth, L.I. Elding, Inorg. Chem. 35 (1996) 5019.
[59] A.D. Hugi, L. Helm, A.E. Merbach, Inorg. Chem. 26 (1987) 1763.
[60] (a) M. Grant, R.B. Jordan, Inorg. Chem. 20 (1981) 55;
(b) T.W. Swaddle, A.E. Merbach, Inorg. Chem. 20 (1981) 4212.
[61] F.C. Xu, H.R. Krouse, T.W. Swaddle, Inorg. Chem. 24 (1985) 267.
[62] A. Cusanelli, U. Frey, D.T. Richens, A.E. Merbach, J. Am. Chem. Soc. 118 (1996) 5265.
[63] J.P. Nordin, D.J. Sullivan, B.L. Phillips, W.H. Casey, Inorg. Chem. 37 (1998) 4760.
[64] I. Rapaport, L. Helm, A.E. Merbach, P. Bernhard, A. Ludi, Inorg. Chem. 27 (1988) 873.
[65] M. Trachtman, G.D. Markham, J.P. Glusker, P. George, C.W. Bock, Inorg. Chem. 40 (2001) 4230.
[66] F.P. Rotzinger, J. Phys. Chem. A 103 (1999) 9345.
[67] F.P. Rotzinger, J. Phys. Chem. A 104 (2000) 6439.
[68] F.P. Rotzinger, J. Phys. Chem. A 104 (2000) 8787.
[69] V. Vallet, U. Wahlgren, B. Schimmelpfennig, Z. Szabo, I. Grenthe, J. Am. Chem. Soc. 123 (2001) 11999.
[70] P.J. Hay, R.L. Martin, G. Schreckenbach, J. Phys. Chem. A 104 (2000) 6259.
[71] M. Hartmann, T. Clark, R. van Eldik, unpublished results.
[72] J. Li, C.L. Fisher, J. Chen, D. Bashford, L. Noodleman, Inorg. Chem. 35 (1996) 4694.
[73] M. Uudsemaa, T. Tamm, Chem. Phys. Lett. 342 (2001) 667.
[74] J. Tomasi, B. Menucci, R. Cammi, M. Cossi, in: G. Naray-Szabo, A. Warshel (Eds.), Theoretical Aspects of Biochemical Reactivity, Kluwer Academic Publishers, Dordrecht, 1997, p. 1.
[75] J.L. Rivail, D. Rinaldi, in: J. Leszczynski (Ed.), Computational Chemistry, Review of Current Trends, World Scientific, New York, 1995, p. 139.
[76] C.J. Cramer, D.G. Truhlar, in: O. Tapia, J. Bertran (Eds.), Solvent Effects and Chemical Reactivity, Kluwer Academic Publishers, Dordrecht, 1996, p. 1.
[77] N.G.J. Richards, in: A.-M. Sapse (Ed.), Molecular Orbital Calculations for Biological Systems, Oxford University Press, New York, 1998, p. 11.
[78] C.J. Cramer, D.G. Truhlar, Chem. Rev. 99 (1999) 2161.
[79] E. Cances, B. Mennucci, J. Chem. Phys. 109 (1998) 249.
[80] E. Cances, B. Mennucci, J. Tomasi, J. Chem. Phys. 109 (1998) 260.
[81] J.L. Rivail, D. Rinaldi, Chem. Phys. 18 (1976) 233.
[82] J.M. Martinez, R.R. Pappalardo, E.S. Marcos, B. Mennucci, J. Tomasi, J. Phys. Chem. B 106 (2002) 1118.
[83] E. Cances, B. Mennucci, J. Tomasi, J. Chem. Phys. 107 (1997) 3032.
[84] B. Mennucci, E. Cances, E.J. Tomasi, J. Phys. Chem. B 101 (1997) 10506.
[85] A. Pullman, in: R. Daudel, A. Pullman, L. Salem, A. Veillard (Eds.), Quantum Theory of Chemical Reactions, vol. II, Reidel Publishing Co, Dordrecht, 1981.
[86] P. Claverie, J.P. Daudey, J. Langlet, B. Pullman, D. Piazzola, M.J. Huron, J. Phys. Chem. 82 (1978) 405.
[87] C.C. Pye, W.W. Rudolph, J. Phys. Chem. A 102 (1998) 9933.
[88] W.W. Rudolph, C.C. Pye, Phys. Chem. Chem. Phys. 1 (1999) 4583.
[89] W.W. Rudolph, R. Mason, C.C. Pye, Phys. Chem. Chem. Phys. 2 (2000) 5030.
[90] M. Pavlov, P.E.M. Siegbahn, M. Sandström, J. Phys. Chem. A 102 (1998) 219.
[91] J.M. Martinez, R.R. Pappalardo, E. Sanchez Marcos, J. Phys. Chem. A 101 (1997) 4444.
[92] U. Cosentino, A. Villa, D. Pitea, G. Moro, V. Barone, J. Phys. Chem. B 104 (2000) 8001.
[93] J. Li, C.L. Fisher, J.L. Chen, D. Bushford, L. Noodleman, Inorg. Chem. 35 (1996) 4694.
[94] F.P. Rotzinger, Helv. Chim. Acta 83 (2000) 3006.
[95] A. Lienke, G. Klatt, D.J. Robinson, K.R. Koch, K.J. Naidoo, Inorg. Chem. 40 (2001) 2352.
[96] E. Clementi, G. Corongiu, J. Quant. Chem. Quant. Biol. Symp. 10 (1983) 31.
[97] M. Wojcik, E. Clementi, J. Chem. Phys. 85 (1986) 5970.
[98] M. Wojcik, E. Clementi, J. Chem. Phys. 86 (1986) 3544.
[99] E. Clementi, J. Chem. Phys. 86 (1986) 6085.
[100] A. Bakker, K. Hermansson, J. Lindgren, M.M. Probst, P.A. Bopp, Int. J. Quant. Chem. 75 (1999) 659.
[101] M.M. Probst, E. Spohr, K. Heinzinger, Chem. Phys. Lett. 161 (1989) 405.
[102] K. Hermansson, M. Wojcik, J. Phys. Chem. B 102 (1998) 6089.
[103] M. Natalia, D.S. Cordeiro, A. Ignazak, J.A.N.F. Gomez, Chem. Phys. 176 (1993) 97.
[104] A. Bakker, K. Hermansson, J. Lindgren, M.M. Probst, P.A. Bopp, Int. J. Quant. Chem. 75 (1999) 659.
[105] A. Lauenstein, K. Hermansson, J. Lindgren, M.M. Probst, P.A. Bopp, Int. J. Quant. Chem. 80 (2000) 892.
[106] M. Magini, Inorg. Chem. 21 (1982) 1535.
[107] A. Musinu, G. Paschina, G. Piccaluga, M. Magini, Inorg. Chem. 22 (1983) 1184.
[108] G. Licheri, A. Musinu, G. Paschina, G. Piccaluga, A.F. Sedda, J. Chem. Phys. 80 (1984) 5308.
[109] J.I. Yagüe, A.M. Mohammed, H. Loeffler, B.M. Rhode, J. Phys. Chem. A 105 (2001) 7646.
[110] T. Yang, S. Tsushima, A. Suzuki, J. Phys. Chem. A 105 (2001) 10439.
[111] D.T. Richens, The Chemistry of Aqua Ions, Wiley, Chichester, 1997.
[112] (a) R.R. Pappalardo, E. Sanchez Marcos, J. Phys. Chem. 97 (1993) 4500;
(b) R.R. Pappalardo, J.M. Martinez, E. Sanchez Marcos, J. Phys. Chem. 100 (1996) 11748;
(c) E. Sanchez Marcos, J.M. Martinez, R.R. Pappalardo, J. Chem. Phys. 105 (1996) 5968;
(d) J.M. Martinez, R.R. Pappalardo, E. Sanchez Marcos, J. Chem. Phys. 109 (1998) 1445;
(e) J.M. Martinez, R.R. Pappalardo, E. Sanchez Marcos, J. Phys. Chem. B 102 (1998) 3272;
(f) J.M. Martinez, R.R. Pappalardo, E. Sanchez Marcos, J. Am. Chem. Soc. 121 (1999) 3175;
(g) J.M. Martinez, R.R. Pappalardo, E. Sanchez Marcos, J. Chem. Phys. 110 (1999) 1669;
(h) J.M. Martinez, J. Hernandez-Cobos, H. Saint-Martin, R.R. Pappalardo, I. Ortega-Blake, E. Sanchez Marcos, J. Chem. Phys. 112 (2000) 2339.
[113] A. Bleuzen, F. Foglia, E. Furet, L. Helm, A.E. Merbach, J. Weber, J. Am. Chem. Soc. 118 (1996) 1669.
[114] C.F. Schwenk, H.H. Loeffler, B.M. Rhode, Chem. Phys. Lett. 349 (2001) 99.
[115] C.F. Schwenk, H.H. Loeffler, B.M. Rhode, J. Chem. Phys. 115 (2001) 10808.
[116] T. Kerdcharoen, B.M. Rhode, J. Phys. Chem. A 104 (2000) 7073.
[117] H.D. Pranowo, B.M. Rhode, J. Phys. Chem. A 103 (1999) 4298.
[118] A. Tongraar, K. Sagarik, B.M. Rhode, J. Phys. Chem. B 105 (2001) 10559.
[119] S. Rast, P.H. Fries, E. Belorizky, A. Borel, L. Helm, A.E. Merbach, J. Chem. Phys. 115 (2001) 7554.
[120] F. Yerley, K.I. Hardcastle, L. Helm, S. Aime, M. Botta, A.E. Merbach, Chem. Eur. J. 8 (2002) 1031.

[121] D. Marx, M. Sprik, M. Parrinello, Chem. Phys. Lett. 273 (1997) 360.
[122] R. Car, M. Parrinello, Phys. Rev. Lett. 55 (1993) 5723.
[123] A. Pasquarello, K. Laasonen, R. Car, D. Vanderbilt, Phys. Rev. Lett. 69 (1992) 1982.
[124] K. Laasonen, A. Pasquarello, R. Car, C. Lee, D. Vanderbilt, Phys. Rev. B 47 (1993) 10142.
[125] I. Persson, P. Persson, M. Sandström, A.S. Ullström, J. Chem. Soc. Dalton Trans. (2002) 1256.